Connexin43 is required for production of the aqueous humor in the murine eye

Mónica R. Calera[1], Heather L. Topley[2], Yongbo Liao[3], Brian R. Duling[3], David L. Paul[2] and Daniel A. Goodenough[1,*]

[1]Department of Cell Biology and [2]Department of Neurobiology, Harvard Medical School, 240 Longwood Avenue, Boston, MA 02115, USA
[3]Department of Molecular Physiology and Biological Physics, University of Virginia, Charlottesville, VA 22908, USA
*Author for correspondence (e-mail: dgoodenough@hms.harvard.edu)

Accepted 7 August 2006
Journal of Cell Science 119, 4510-4519 Published by The Company of Biologists 2006
doi:10.1242/jcs.03202

Summary

Connexin43 is a major component of the gap junctions between pigmented and non-pigmented cells of the double-layered epithelium in the ciliary body of the eye. We directly tested the hypothesis that gap junctions play a crucial role in the production of the aqueous humor by inactivating the *GJA1* (connexin43) gene in the pigmented epithelium with cre-loxP technology. To accomplish this, we crossed a line expressing *cre* recombinase driven by the nestin promoter and a line with floxed connexin43 alleles. Resultant lines exhibited loss of connexin43 from the pigmented epithelium, iris, retinal pigment epithelium and the lens. We observed plasma proteins in the aqueous humor and pathological changes consistent with a loss of intraocular pressure. As the ciliary body is responsible for aqueous humor production, these data support the hypothesis that the gap junctions between pigmented and non-pigmented epithelium are necessary for production of the aqueous humor that is in turn required for the generation of normal intraocular pressure and nourishment of the postnatal lens. The loss of connexin43 expression in the iris correlated with a separation of the posterior pigmented epithelium from the anterior myoepithelium and with meiosis, possibly resulting from a loss of function of the dilator pupillae.

Supplementary material available online at
http://jcs.biologists.org/cgi/content/full/119/21/4519/DC1

Key words: Gap junction, Connexin43, Ciliary epithelium, Aqueous humor

Introduction

The ciliary epithelium of the eye consists of a double-layer of epithelial cells. The pigmented epithelium (PE) rests on the connective tissue stroma and the non-pigmented epithelium (NPE) is polarized with its basal lamina facing the posterior chamber of the eye. The PE and NPE interact via their apical membranes with gap junctions (Oh et al., 1994; Raviola and Raviola, 1978), which have been shown by immunofluorescence to include two members of the connexin gene family, connexin43 (Cx43) and Cx40 (Coffey et al., 2002). The NPE forms tight junctions delineating a boundary between the blood and the aqueous humor as part of the blood-retina barrier (Raviola, 1974). The combined ion transporters and pumps located in the ciliary epithelium provide the source of the aqueous humor, most of which leaves the eye by crossing the endothelial layers investing the trabecular meshwork and the canal of Schlemm. This aqueous outflow likely requires the positive pressure generated by secretion from the ciliary epithelium as experimental lowering of intraocular pressure by paracentesis or urea results in the backflow of blood proteins from episcleral veins into the aqueous humor (Raviola, 1974; Raviola, 1976).

Current models identify three phases of aqueous humor secretion by the ciliary epithelium (Civan and Macknight, 2004). First, NaCl enters the PE from the stroma via paired Na^+/H^+ and Cl^-/HCO_3^- antiporters (McLaughlin et al., 1998). Second, NaCl moves through gap junctions into the NPE. Third, NaCl is actively secreted into the aqueous humor by basolateral Na^+/K^+ ATPase and Cl^- channels (Civan and Macknight, 2004). Water following this NaCl movement can also pass from PE to NPE via gap junctions (Walker et al., 1999), and exit the NPE to the posterior chamber using basolaterally located aquaporin4 (Yamaguchi et al., 2006). The secretion of NaCl into the posterior chamber may be partially regulated by purinergic A3 receptors since knockout of A3ARs reduces mouse intraocular pressure (IOP) (Avila et al., 2002). It has been shown that octanol (Stelling and Jacob, 1997) and heptanol (Do and Civan, 2004; Wolosin et al., 1997) block gap junctions joining the PE and NPE. However, these reagents are non-specific and heptanol has been shown to cause cell volume changes (Wolosin et al., 1997) as well as decreases in the transepithelial resistance (Do and To, 2000), indicating additional effects on the tight junctions regulating the paracellular pathway. As there are no specific inhibitors of connexins, this problem must be approached using mouse genetics.

Targeted deletion of Cx43 in mice causes no gross structural changes in the prenatal eye (White et al., 2001) but animals die postnatally from cardiac abnormalities precluding further study (Reaume et al., 1995). However, there is genetic evidence that Cx43 mutations may affect postnatal intraocular pressure. Oculo-dento-digital dysplasia (ODDD) is a heritable disease affecting many organ systems that is caused by mutations in Cx43 (Loddenkemper et al., 2002; Paznekas et al., 2003). ODDD patients with different Cx43 mutations show variable

eye disorders (Debeer et al., 2005) including glaucoma (Vasconcellos et al., 2005) [see also Table 3 of Loddenkemper et al. (Loddenkemper et al., 2002)]. A mouse model of ODDD with a G60S mutation in Cx43 also shows eye abnormalities (Flenniken et al., 2005).

To overcome the perinatal lethality observed in the constitutive Cx43 knockout (Reaume et al., 1995), we produced a conditional knockout with spatially restricted deletion of *GJA1* (Cx43) using the nestin promoter to drive the expression of *cre* recombinase (nestin-*cre*). Although most often associated with the nervous system (Thuret et al., 2004), nestin expression has been reported in the lens epithelium and primary lens fibers, in the developing ciliary body (including the presumptive iris) and in the retina and optic nerve (Mayer et al., 2003; Yang et al., 2000). During development, nestin mRNA and protein was found in the lens vesicle at E10.5 in addition to the optic disk and nerve, but did not appear in the ciliary body until E17.5 (Yang et al., 2000). To verify ocular expression, we crossed a nestin-*cre* line with the ROSA26 reporter line (Soriano, 1999). Consistent with endogenous nestin expression, we observed β-galactosidase activity in postnatal nestin-*cre*/ROSA26 animals in the distal retina, ciliary epithelium, iris and lens, indicating the expression of cre recombinase in these structures.

A mouse line carrying loxP sites flanking exon 2 of the Cx43 gene (Liao et al., 2001) was crossed with the nestin-*cre* line. Nestin-*cre*/Cx43$^{flox/flox}$ mice displayed a loss of immunohistochemically detectable Cx43 in the tissues where β-galactosidase was detected in the nestin-*cre*/ROSA26 line. Central to this study, the nestin-*cre*/Cx43$^{flox/flox}$ mice showed a consistent postnatal loss of Cx43 from the pigmented epithelium of the ciliary body, potentially reducing the intercellular channels between the PE and NPE. In this study, we document ocular abnormalities caused by the loss of Cx43 due to nestin-*cre* activity in the postnatal mouse that are consistent with a requirement for gap junctions between the PE and NPE for the production of the aqueous humor.

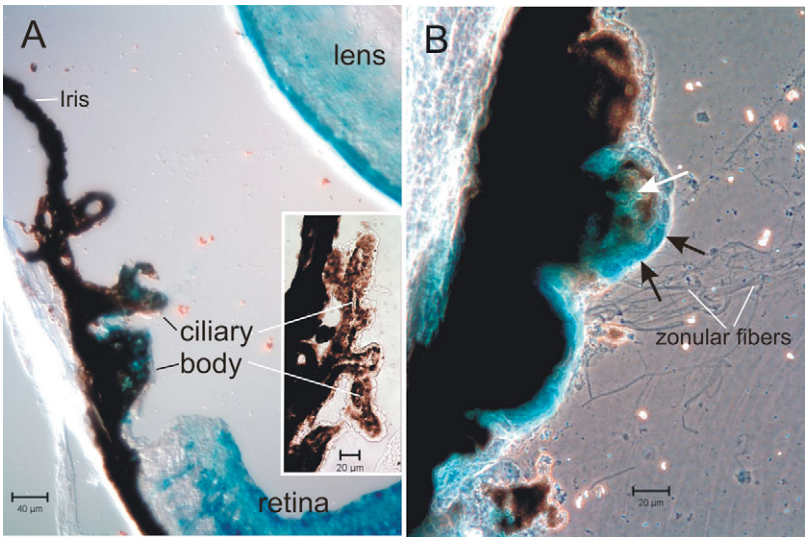

Fig. 1. Localization of the β-galactosidase reaction product in 5.5-week-old nestin-*cre*/ROSA26 mice. (A) At low power, the blue reaction product is evident in the retina, lens and ciliary body. Owing to the heavily pigmented PE and iridal epithelial cells, the reaction product is difficult to see in these locations. (Inset A) Control specimen showing no reaction product. (B) At higher magnification, β-galactosidase activity is clearly visible in the NPE cells (black arrows) and, with favorable planes of section, in the PE cells (white arrows). The zonular fibers joining the ciliary body to the lens are indicated.

Results

The nestin-*cre* transgene is expressed in the mouse eye

To inactivate Cx43 in the ciliary epithelium of Cx43$^{flox/flox}$ mice, we employed a transgenic mouse line that expressed *cre* recombinase under the control of the nestin promoter, as nestin expression has been reported in this organ (Mayer et al., 2003; Yang et al., 2000). To determine if the nestin-*cre* transgene was expressed in the ciliary processes, we evaluated β-galactosidase activity in mice originating from crosses between nestin-*cre* [B6.Cg-Tg(Nes-cre)1Kln/J; Jackson Laboratories, Bar Harbor, ME] and ROSA26 reporter (Soriano, 1999) mouse lines. As shown in Fig. 1A, β-galactosidase activity was detected in the ciliary processes, the retina and the lens epithelium from this 5.5 week-old mouse. Owing to the pigmentation of PE and iridal epithelial cells, the blue reaction product was difficult to see in these locations at low magnification (Fig. 1A). However, at higher magnification (Fig. 1B), reaction product was clearly visible in the NPE cells (black arrows) and in the PE cells with favorable planes of section (white arrows). Thus, the nestin-*cre* transgenic mouse line was an appropriate tool to inactivate Cx43 for study of aqueous secretion.

Cx43 protein levels are decreased by nestin-cre in pigmented cells in the ciliary body, iris and retinal pigment epithelium of Cx43$^{flox/flox}$ mice

To determine if Cx43 expression in eye structures was abolished by nestin-*cre* in Cx43$^{flox/flox}$ mice, we performed immunostaining using the Sigma anti-Cx43 antibody. Comparisons were made between the *cre*-positive heterozygotes (Cx43$^{+/flox}$) and homozygotes (Cx43$^{flox/flox}$). Specimens were studied using paraffin-embedded sections. At E16-18, eye development appeared normal in heterozygote controls (Fig. 2B) and in the conditional KO (Fig. 2D). In the heterozygote, Cx43 immunoreactivity (Fig. 2A) was present in the ciliary epithelium (and presumptive iris), lens, cornea, and retinal pigment epithelium (RPE). By contrast, the homozygote (Fig. 2C) exhibited a notable reduction in the staining of the ciliary epithelium and a complete loss of staining in the RPE.

Unexpectedly, Cx43 immunostaining was observed in the differentiating lens fibers in both *cre* positive Cx43$^{+/flox}$ and Cx43$^{flox/flox}$ lines. To verify the authenticity of this signal, Cx43$^{-/-}$ and Cx43$^{+/-}$ E15 embryos (Reaume et al., 1995) were prepared for immunostaining in paraffin sections using the Sigma anti-Cx43 antibody. Fig. 3 reveals lens fiber staining in both Cx43$^{+/-}$ and Cx43$^{-/-}$ lens fibers, demonstrating that in protease-treated, paraffin sections, the lens fiber staining was non-specific. However, the staining seen in the Cx43$^{+/-}$ ciliary body (CB in Fig. 3A) was absent in the Cx43$^{-/-}$specimen (Fig. 3B),

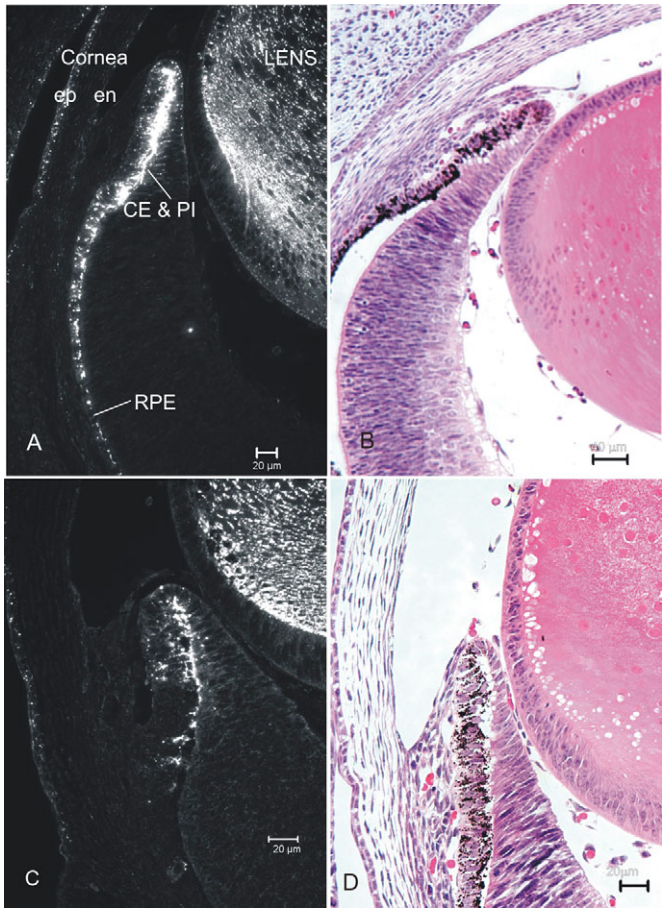

Fig. 2. Nestin-*cre* reduces Cx43 expression in the ciliary epithelium and iris by embryonic day 16-18. Eyes from nestin-*cre*/Cx43$^{+/flox}$ (A,B) and nestin-*cre*/Cx43$^{flox/flox}$ (C,D) mice were harvested, treated and sectioned as described in Materials and Methods section. Photomicrographs of immunostaining using anti-Cx43 antibody (A,C) and H and E stained (B,D) sections from the same specimens were taken. (A) In the heterozygote, Cx43-positive staining is seen in the ciliary epithelium (CE) and presumptive iris (PI) and in the corneal epithelium (ep) and endothelium (en) and the retinal pigment epithelium (RPE). The lens staining is non-specific (see Fig. 3). (C) In the homozygote, a reduction of staining is evident in the ciliary epithelium and presumptive iris. Bars, 20 μm.

confirming that the immunofluorescent signal represents bona fide Cx43 in this structure. To document whether Cx43 was removed from the lens as expected from the ROSA26 data (Fig. 1), lens capsules were stripped from 6-week-old Cx43$^{+/flox}$ and Cx43$^{flox/flox}$ lenses, mounted directly on microscope slides following paraformaldehyde fixation, and stained with anti-Cx43 antibodies from different sources (Chemicon or Invitrogen/Zymed). Fig. 4 shows that the junctional staining observed in the heterozygotes (4A) was absent in the homozygotes (4C), indicating that nestin-*cre* expression eliminates Cx43 expression in the lens. As the Chemicon and Zymed antibodies were not suitable for staining paraffin sections, the data obtained using the Sigma antibody are presented in this study to take advantage of the increased resolution available with paraffin sections, mindful that the lens staining is not valid.

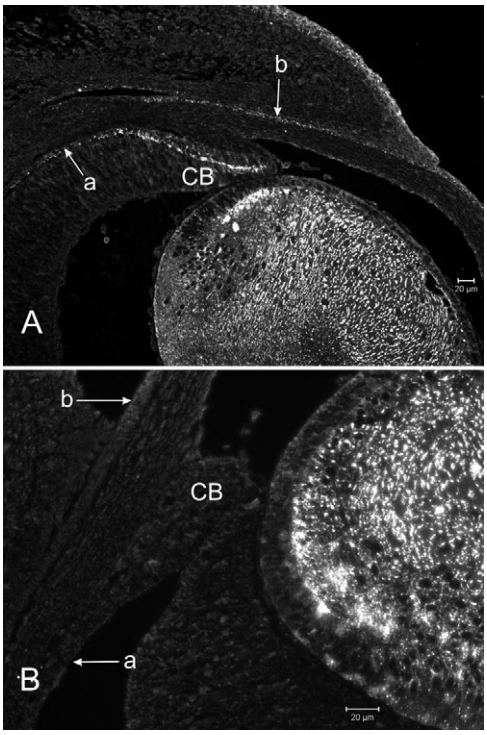

Fig. 3. Immunohistochemistry on paraffin sections of Cx43$^{+/-}$ (A) and Cx43$^{-/-}$ (B) eyes from E15 mouse embryos using the Sigma anti-Cx43 reagent. (A) In the heterozygote, strong signal is seen in the lens, ciliary body (CB), RPE (arrows, a), corneal epithelium (arrows, b). (B) In the homozygous Cx43 knockout, the lens staining persists, indicating a non-specific signal. The staining is completely removed, however, from the ciliary body, cornea and RPE.

At birth, a characteristic change in the Cx43 distribution was evident in the ciliary epithelium (Fig. 5A,B). Homozygotes (Fig. 5B) exhibited a dramatic loss of Cx43 immunoreactivity in the PE compared with controls (Fig. 5A). Cx43-positive plaques were still evident in the homozygote NPE but at a reduced frequency compared with controls. Cx43 staining remained comparable in the cornea between the two mouse lines. The selective loss of Cx43 immunostaining in the PE persisted at all later stages, as illustrated in at higher magnification in P14 animals in Fig. 5C,D. The loss of Cx43 from the PE was also confirmed in frozen sections using the Sigma and Invitrogen/Zymed antisera (see supplementary material Fig. S1).

Loss of Cx43 results in major alterations in eye structure

To determine whether loss of Cx43 affected the general structure of the eye, we examined H and E stained paraffin sections. At P7 there were dramatic histological differences between homozygotes and controls (Fig. 6A,B). Homozygous eyes (Fig. 6B) contained precipitated material in anterior (double asterisk) and posterior chambers (triple asterisk) and vitreous bodies together with a separation of the iris into two layers (single asterisk). The ciliary epithelium in the homozygote showed variable areas of separation between the PE and NPE not seen in the heterozygotes (insets, Fig. 6B, arrows). Immunofluorescence microscopy confirmed loss of

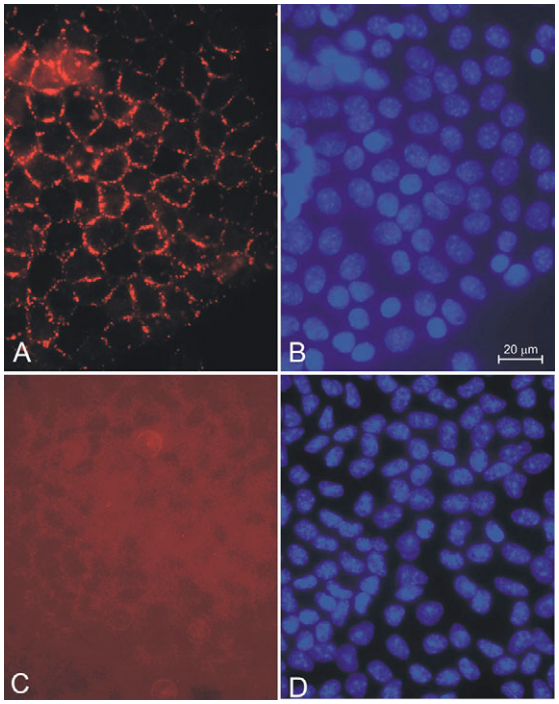

Fig. 4. Fluorescence images of stripped capsules with attached lens epithelial cells from 6-week-old nestin-*cre* positive $Cx43^{+/flox}$ (A,B) and $Cx43^{flox/flox}$ (C,D) lenses. Cx43 is stained with the Chemicon anti-Cx43 reagent (A,C) and nuclei are visualized with Hoechst staining (B,D). There is a loss of the punctate gap junctional staining in the homozygote (C) demonstrating loss of Cx43 from the lens epithelium.

Cx43 immunoreactivity from the PE but not the NPE (compare Fig. 6C with D). In addition, the iridal epithelium also lost immunostaining (Fig. 6C,D), although Cx43 staining remained in the sphincter of the iris (data not shown).

At 2 weeks and older, gross anatomical differences between homozygotes and controls could be discerned. Homozygotes were microphthalmic (smaller eyes) and enophthalmic (loss of eye protrusion) relative to controls (see supplementary material Fig. S2A,B). Following euthanasia and enucleation, the nestin-*cre*/$Cx43^{flox/flox}$ eyes were grossly flaccid, smaller and usually presented with an off-optical axis, asymmetric meiosis (see supplementary material Fig. S2C,D). The pattern of Cx43 loss in the ciliary epithelium remained evident (Fig. 5C,D). Histological examination of the homozygous eye at 5 weeks of age (Fig. 7) revealed a dramatic loss of the vitreal space with concomitant adhesion of the retina to the posterior surface of the lens and changes in the layering of the retina (Fig. 7A). Also noted were disorganization of the bilayered structure of the ciliary epithelium and evidence of lens fiber fusion and distortion of the lenticular structure (Fig. 7B).

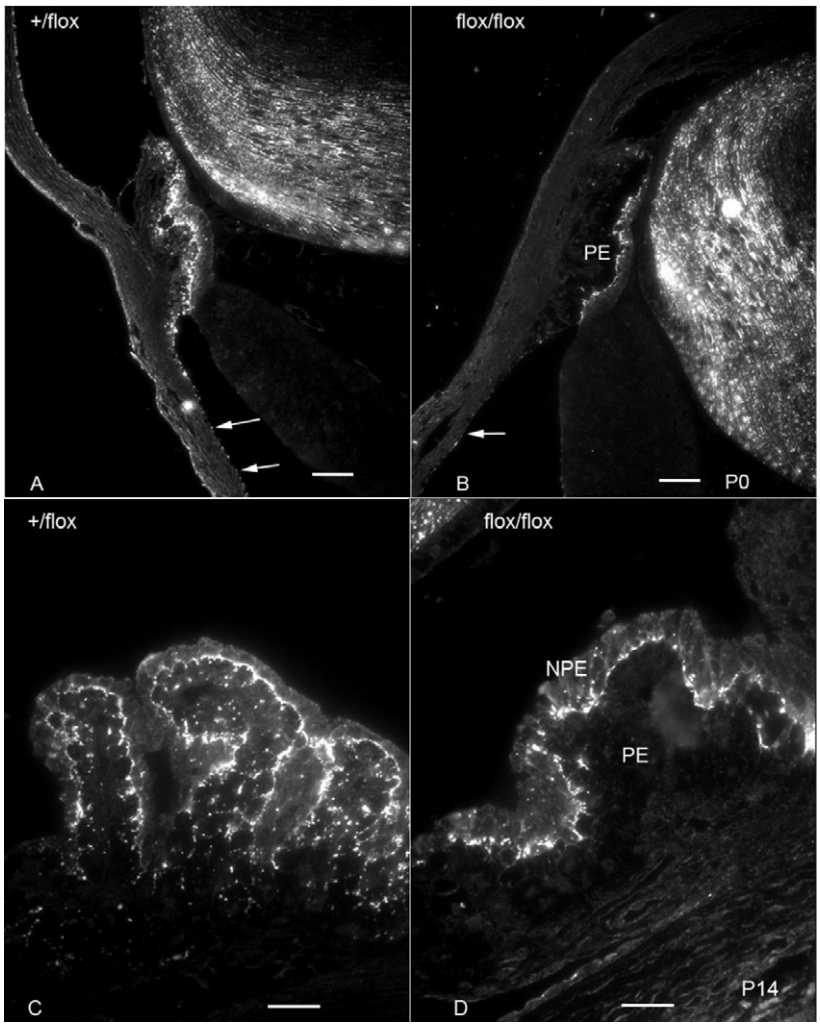

Loss of Cx43 causes back-diffusion of blood proteins into the ocular space

One explanation for the flaccid, microphthalmic eyes in the homozygote would be that loss of Cx43 from the PE affects ion and water flow across the ciliary epithelium leading to a loss of intraocular pressure (IOP). Loss of IOP would be expected to promote back-diffusion of plasma proteins from episcleral veins and the canal of Schlemm that could account for the precipitate observed in anterior chamber. It has been demonstrated in the monkey (Raviola, 1974) that a rapid decrease in intraocular pressure (IOP) caused by the acute removal of the aqueous humor results in leakage of proteins from episcleral veins into the anterior chamber.

Fig. 5. Cx43 expression is abolished by nestin-*cre* in the pigmented epithelium of the ciliary body and retinal pigment epithelium of $Cx43^{flox/flox}$ mice. At P0 (B) and at P14 (D) a loss of detectable Cx43 staining is observed in the pigmented epithelium (PE) but not in the non-pigmented epithelium (NPE) of the ciliary processes in the nestin-cre^{+}/$Cx43^{flox/flox}$ (B,D) as compared with the nestin-cre^{+}/$Cx43^{+/flox}$ mice (A,C). Cx43 staining in the homozygote is also lost in the retinal pigment epithelium (arrows, A,B). There is no apparent change in Cx43 immunoreactivity in the lens due to the non-specific staining illustrated in Fig. 3. Bars, 50 μm (A,B); 20 μm (C,D).

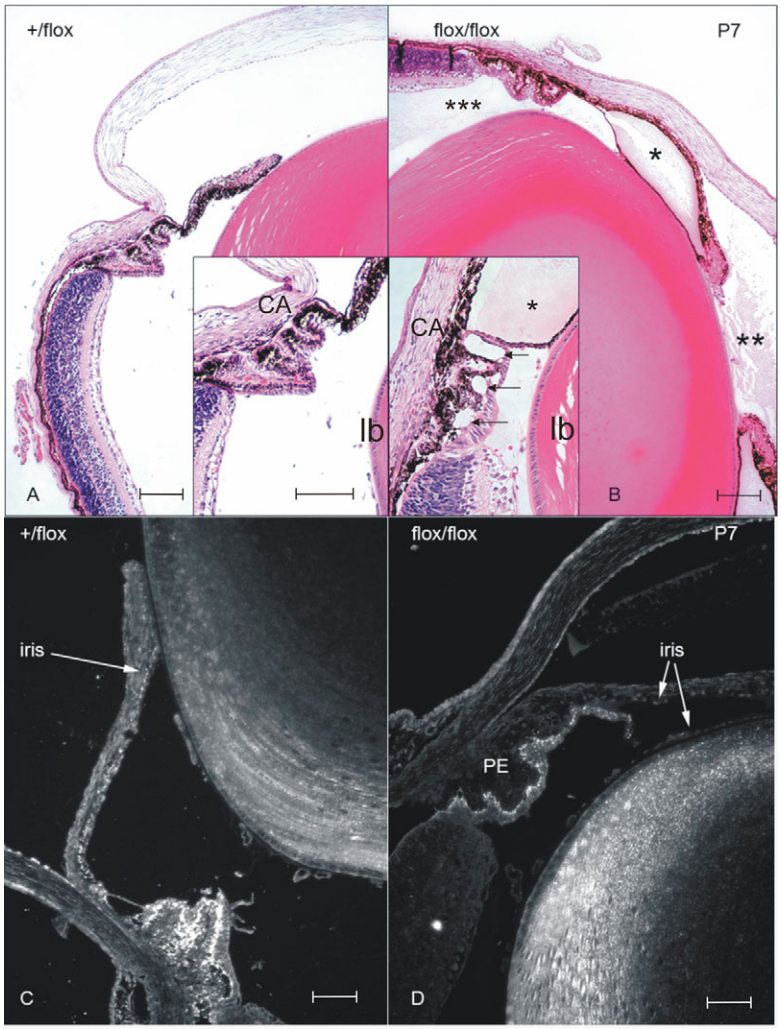

Fig. 6. Eyes from Cx43-deficient mice display structural changes. Eye sections from nestin-*cre*/Cx43$^{+/flox}$ (A,C) and nestin-*cre*/Cx43$^{flox/flox}$ (B,D) mice at P7 were used for H and E staining (A,B) and anti-Cx43 immunostaining (C,D). (A,B) Clear changes are evident in the anterior eye in the homozygote at 1 week of age. The posterior pigmented epithelium of the iris detached from the myoepithelium, leaving a precipitate-filled space (B, asterisk). A precipitate is also visible in the anterior chamber (B, double asterisk) and in the posterior chamber adjacent to the ciliary body and ora serrata (B, triple asterisk). The insets A and B compare the ciliary body, lens bow (lb) and iris close to the corneal angle (CA). In the homozygote, there is a variable separation of the PE from the NPE leaving clear vacuoles (arrows, inset B). (C,D) Immunostaining reveals a loss of Cx43 from the pigmented epithelium (PE) and from the iris (which has split, leaving the posterior pigmented epithelium on the surface of the lens. Bars, 100 μm (insets at the same magnification).

A chronic loss of IOP in the homozygous mouse might produce a similar effect. To test this possibility, aqueous humor was collected from the anterior chamber of heterozygotes and homozygotes and analyzed by SDS-PAGE and mass spectroscopy. As shown by silver-stained SDS gel analysis (Fig. 8) the homozygote aqueous contained proteins not detected in the heterozygote. Seven bands were excised and analyzed by mass spectroscopy (NC 1-7) and the results presented in the supplementary material Table S1. Only proteins showing at least two matching peptides were scored in this analysis, providing a conservative list. Plasma proteins composed 55% of the total number of identified proteins, consistent with the notion that loss of Cx43 results in reduced IOP. Neither alpha nor beta hemoglobin was detected, indicating no contamination of whole blood in our samples (Rohde et al., 1998).

Alternatively, the presence of plasma proteins in the aqueous humor could be due to a loss of integrity of the blood-aqueous barrier. To test this possibility, horseradish peroxidase (HRP) permeability studies (Karnovsky, 1967) were carried out. HRP was introduced into the vascular system by injection into the inferior vena cava and allowed to circulate for five-minutes before animal sacrifice. Localization of HRP in the eye in heterozygous animals followed the distribution published for the monkey (Raviola, 1974). At the light microscopic level, HRP reaction product stained blood vessels in the stroma of the ciliary body and iris in both Cx43$^{+/flox}$ (Fig. 9A) and Cx43$^{flox/flox}$ (Fig. 9B). HRP reaction product was

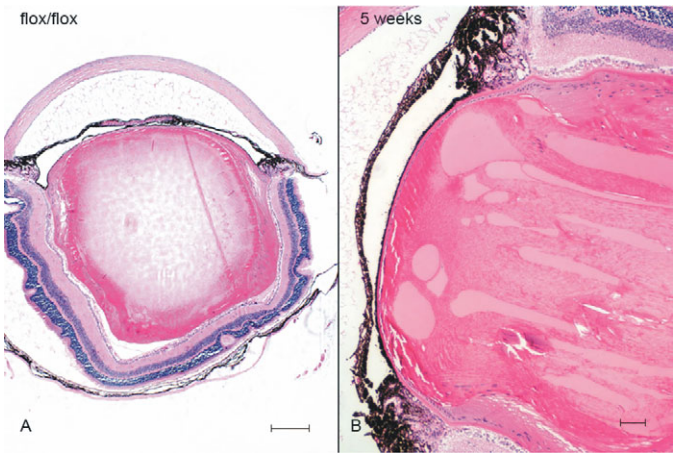

Fig. 7. Ablation of Cx43 by nestin-*cre* causes a complete loss of the vitreal space and alterations in the ciliary body, retina and lens. (A) At 5 weeks of age, the nestin-*cre*$^{+}$/Cx43$^{flox/flox}$ eye shows a precipitated material in the anterior chamber beneath the cornea. The vitreal space is almost completely absent, with the lens in close apposition to the inner limiting membrane of the retina. The iris remains separated into two layers, the posterior pigmented epithelium adherent to the anterior surface of the lens and to the vitreal side of the ciliary body. The retinal layers are wavy and non-uniform in thickness. (B) At higher power, clear lakes have appeared in the lens where lens fibers have fused. The ciliary body appears disorganized, with a loss of recognizable ciliary processes. The posterior pigmented epithelium of the iris can be seen more clearly adherent to the anterior surface of the lens. Both A and B are sectioned para-saggitally to the pupil. Bars, 100 μm (A); 50 μm (B).

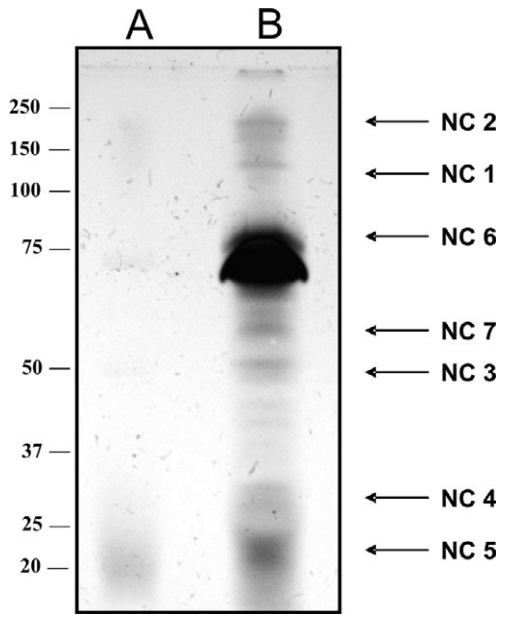

Fig. 8. Silver-stained SDS-PAGE of aqueous humor from Cx43$^{+/flox}$ (lane A) and Cx43$^{flox/flox}$ (lane B) reveals increased protein levels in the homozygote. Numbers on the right indicate the locations of the molecular weight standards. Arrows NC 1-7 indicate locations were the gel was sampled for mass spectroscopy. The MS results are shown in the supplementary material Table S1, corresponding to each of the NC samples.

evident in the anterior chamber of the homozygote (Fig. 9B) that was not evident in the heterozygote (Fig. 9A) in the location where the precipitated material was seen in paraffin sections.

To determine if loss of Cx43 resulted in loss of tight junction barrier function resulting in leakage of tissue protein into the aqueous humor, HRP reaction product was localized at the electron microscope level. In the ciliary epithelium of 2.5-week-old animals, HRP was detected at the PE/NPE interface (Fig. 10), but tight junctions (Fig. 10, insets) prevented its diffusion into the intercellular spaces between the NPE cells or into the posterior chamber in both heterozygotes and homozygotes. In addition, peroxidase activity remained sequestered within retinal and iridal blood vessels, indicating the blood-aqueous-retinal barrier was intact (insets, Fig. 9B). Given that the system of tight junctions protecting the aqueous humor was still intact, the likely source of the blood proteins (and the HRP) in the aqueous was back-diffusion from episcleral veins due to insufficiency in aqueous production. Thus, a chronic loss of aqueous pressure in the mouse due to removal of Cx43 from ocular organs mimics the back-diffusion of blood proteins seen following acute paracentesis in the monkey (Raviola, 1974).

While Cx43 is removed from the PE, Cx43 staining was still observed close to the PE/NPE interface (see Fig. 5D). To determine if removal of Cx43 from the PE resulted in the loss of morphologically recognizable gap junctions, the interface was studied using electron microscopy.

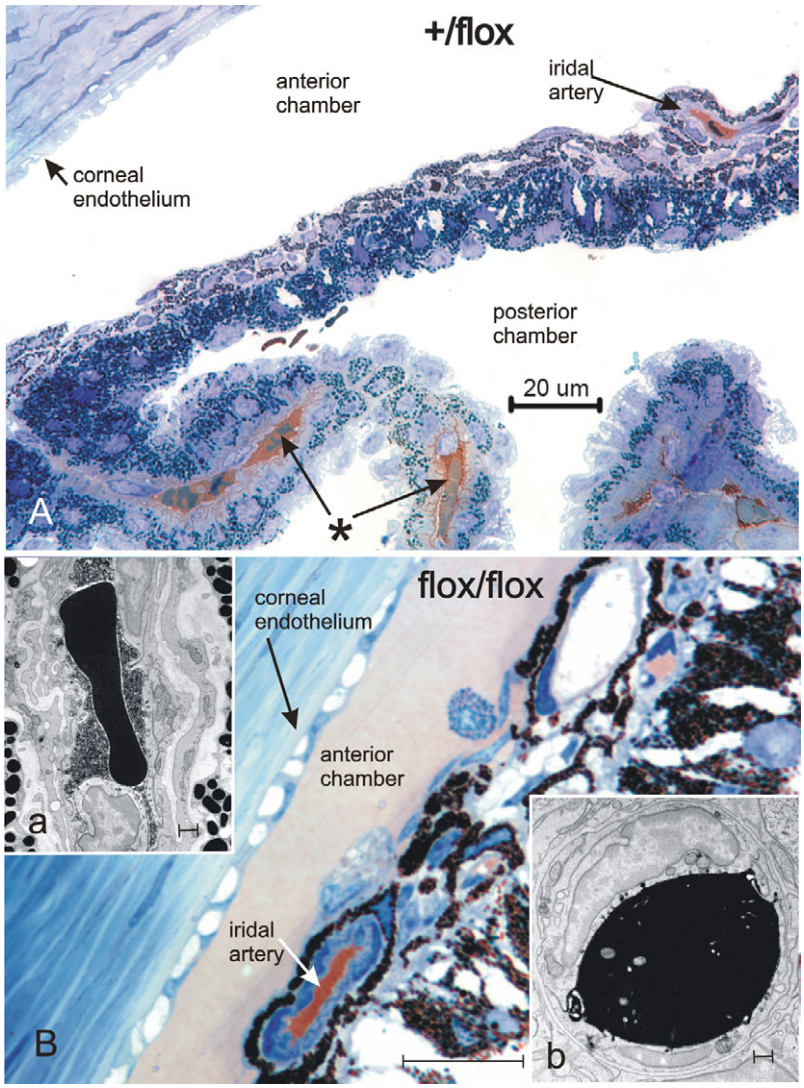

Fig. 9. Cx43 inactivation results in back-diffusion of plasma proteins from the veins into the eye chambers. (A) HRP reaction product stains the subendothelial connective tissue and vasculature in the stroma of the ciliary body (asterisk arrows) of a nestin-*cre*$^{+}$/Cx43$^{+/flox}$ mouse as visualized by light microscopy. The HRP is also visible in an iridal artery. (B) In a nestin-*cre*$^{+}$/Cx43$^{flox/flox}$ mouse, the HRP has entered the anterior chamber where H and E staining revealed a precipitate (see Fig. 6B and Fig. 7). HRP was contained in iridal blood vessels, notably in an indicated artery. Inset: electron microscopy demonstrates that the blood-ocular barrier at the level of the iridal (inset a) and retinal (inset b) blood vessels was not disrupted by Cx43 removal. These images show capillaries exhibiting containment of the HRP reaction product within the lumen of the vessel. The iridal vessel contains a peroxidase-positive erythrocyte. Bars, 20 μm (A); 10 μm (B); 500 nm (insets).

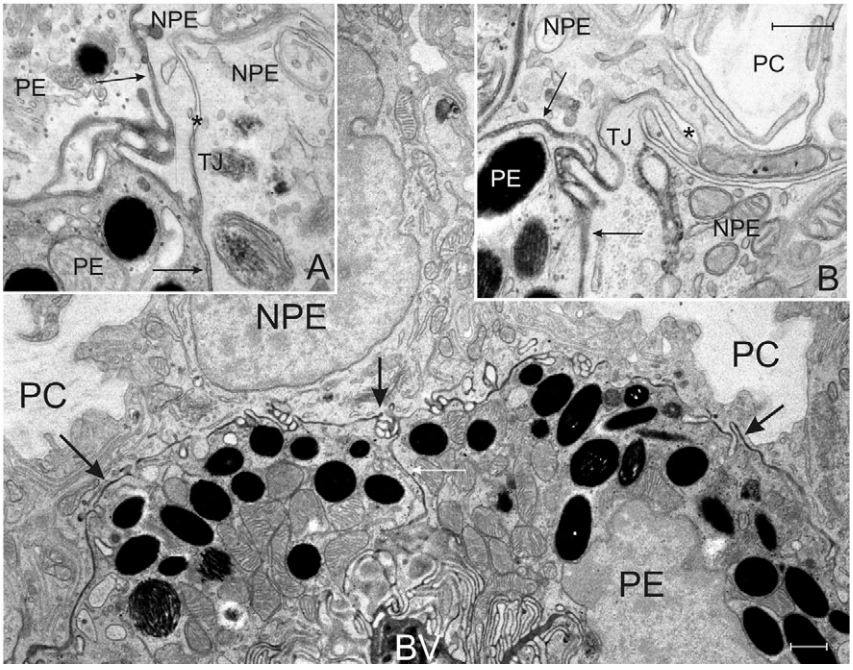

Fig. 10. Tight junctions are functional at 2.5 weeks in the Cx43-deficient mice. The figure and inset B are from a nestin-*cre*$^{+}$/Cx43$^{+/flox}$ animal, and inset A is from a nestin-*cre*$^{+}$/Cx43$^{flox/flox}$ mouse. Five minutes following intravenous HRP injection, the reaction product can be seen by electron microscopy in stromal blood vessels of the ciliary body (BV), in the intercellular spaces between pigmented epithelial (PE) cells (white arrow) and at the interface between the (PE) and non-pigmented epithelium (NPE) (black arrows). In the insets, HRP diffusion can be seen blocked by tight junctions (TJ) so that no reaction product can be seen in the intercellular spaces either between the NPE cells (asterisks) or in the posterior chamber (PC). Bars, 500 nm.

Surveying 200 μm of PE/NPE interface, 23 clearly distinguishable gap junctions were found in the heterozygote (a small sample shown in Fig. 11A) consistent with the literature (Raviola et al., 1980; Raviola and Raviola, 1978). In the homozygote, however, scanning of a comparable 200 μm length revealed no gap junctions (Fig. 11B), although small or obliquely sectioned junctions would not have been visible in either specimen. Thus, we feel it likely that the remaining Cx43 staining visible near the PE/NPE interface comes from NPE/NPE gap junctions that tend to cluster near the tight junctions at the apico-lateral surfaces (see white arrows in Fig. 11).

Previous studies have identified Cx40 as also being present at the PE/NPE interface (Coffey et al., 2002). It is possible that removal of Cx43 resulted in significant changes in Cx40 that contributed to the observed ocular pathology. We have studied the distribution of Cx40 using two antisera. Using one reagent (Simon et al., 1998), we were unable to detect Cx40 staining in either WT or nestin-*cre*/Cx43$^{+/-}$ ciliary epithelia. Using an Alpha Diagnostic International anti-Cx40 reagent, we observed staining at the PE/NPE interface, similar to that reported by Coffey et al. (Coffey et al., 2002). However, this reagent produced an indistinguishable signal in Cx40$^{-/-}$ ciliary bodies, indicating that this staining was non-specific (see supplementary material Fig. S3). Coffey et al. used a completely different antiserum (Yeh et al., 1997), and so comparisons here are not meaningful. As we have been unable to confirm the presence of Cx40, its involvement in aqueous production will require additional study using in-situ hybridization methodologies.

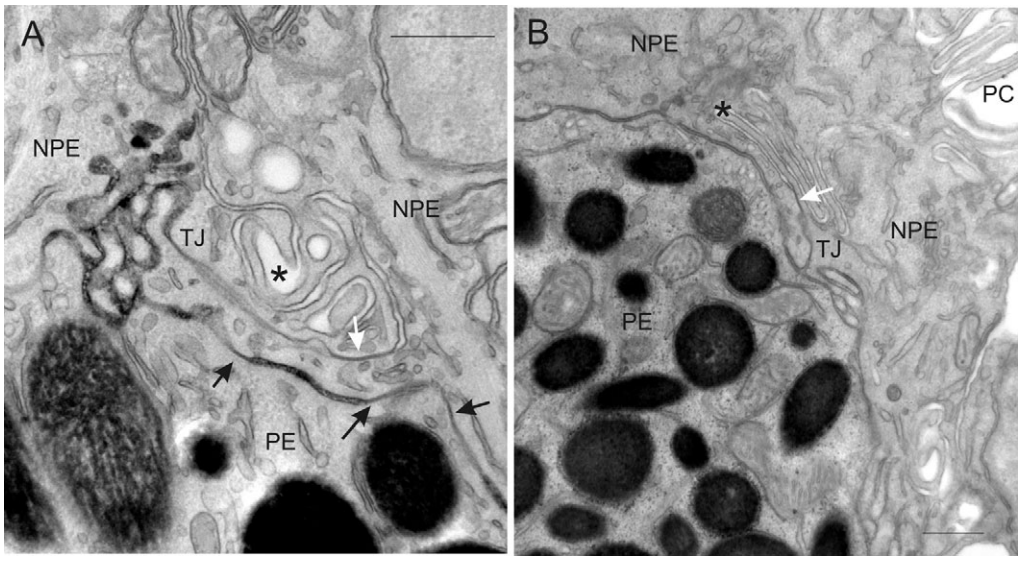

Fig. 11. A representative example of the PE/NPE interface in nestin-*cre*$^{+}$/Cx43$^{+/flox}$ (A) and nestin-*cre*$^{+}$/Cx43$^{flox/flox}$ (B) ciliary bodies of 2.5-week-old animals. In the heterozygote, gap junctions between PE and NPE are very frequent, as indicated by the black arrows. Less frequently, gap junctions can also be observed between NPE cells (white arrows). In the homozygote, gap junctions are not observed at the PE/NPE interface. As described in Fig. 10, tight junctions (TJ) can also be seen limiting the diffusion of HRP between the NPE cells (asterisks).

Discussion

Since Cx43 was removed from a variety of structures, the complex ocular phenotypes described here likely result from changes in communication involving multiple cell types. However, the loss of secretion of aqueous humor is likely due to the lack of gap junctional intercellular communication between PE and NPE cells of the ciliary epithelium. This loss of communication would interdict the postulated second phase of aqueous secretion (Civan and Macknight, 2004), interrupting the diffusion of NaCl and water from the PE into the NPE, thus removing substrate from the basolaterally located Na^+/K^+ATPase and Cl^- channels. While the NPE continued to express Cx43 in nestin-*cre*/Cx43$^{flox/flox}$ ciliary bodies, the PE lost all detectable expression, thus denying the assembly of a complete Cx43 PE/NPE heterologous intercellular channel. Consistent with this hypothesis, we observed a loss of morphologically recognizable gap junctions from the PE/NPE interface by electron microscopy. With no aqueous secretion, intraocular pressure would fall, resulting in grossly notable ocular flaccidity and enophthalmos.

Loss of intraocular pressure in the monkey eye results in back-diffusion of blood proteins via the aqueous outflow pathway: from episcleral veins to the canal of Schlemm, crossing the endothelium of the canal and then the endothelium investing the trabecular meshwork, and finally entering the anterior chamber and the remainder of the eye (Raviola, 1974). Our HRP tracer studies and mass spectroscopy analysis of mouse aqueous humor indicated that a similar phenomenon occurred in nestin-*cre*/Cx43$^{flox/flox}$ animals, giving rise to the precipitate found in various intraocular spaces. We found plasma proteins in the aqueous humor and that intravenous HRP could gain access to intraocular spaces in the nestin-*cre*/Cx43$^{flox/flox}$ eyes. As the tight junctions between NPE cells and retinal and iridal endothelial cells that constitute the blood-ocular barrier remained intact, the route of plasma protein access most likely involved the episcleral veins and the canal of Schlemm. It is noted that blocking the episcleral veins in the outflow pathway by cauterization results in the converse phenotype: increased intraocular pressure and glaucoma (Ruiz-Ederra and Verkman, 2006).

While the loss of Cx43 from the ciliary epithelium provides the most likely explanation of the lower aqueous humor production, it is also true that nestin-*cre* activity resulted in the loss of Cx43 from the AME and PPE of the iris, the RPE and the lens. Given the asynchronous loss of Cx43 from these tissues reviewed in the Introduction, it is possible that the ciliary epithelium experienced the loss of key developmental signals resulting in improper development of this organ. Thus, the lack of production of sufficient aqueous humor to maintain intraocular pressure and normal aqueous outflow may have had contributions from other cellular pathologies independent of the loss of Cx43 from the PE/NPE interface. For example, it has been reported in the chick (Pearson et al., 2005) that Cx43 hemichannels in the RPE release ATP that stimulates proliferation of neural retinal progenitor cells. Parenthetically, we have not seen any differences in retinal thickness in *cre*-positive Cx43$^{flox/flox}$ animals before 3 weeks of age (or in embryonic Cx43$^{-/-}$ retinas) indicating that the stimulation of proliferation in the retina may not operate in the mouse. Nevertheless, other key signaling functions dependent on Cx43 could result in differences in the development and subsequent physiology of the ciliary epithelium that contributed to the reported ocular pathology.

The gross development of the lens continued normally up to 2 weeks following birth in the absence of Cx43. However, following that time, the lens showed progressive pathology. This may have been due to the loss of Cx43 from the lens epithelium or to a failure of aqueous humor production. The postnatal lens receives its nutrients via the aqueous humor following the loss of the tunica vascula lentis (TVL). While the TVL shows signs of apoptotic regression as early as E17.5 (Mitchell et al., 1998), the structure persists until close to eye opening at P12-14 (Ito and Yoshioka, 1999). Consistent with this timing, the lens in the nestin-*cre*/Cx43$^{flox/flox}$ eye appeared grossly normal through P14. Following this time, variable changes in lens shape and the presence of nuclear cataracts became evident, up to gross fusion of lens fibers and lens opacities at 5 weeks. In the mouse, therefore, it is possible that eye opening corresponds to the point when the lens becomes completely dependent on the aqueous humor. If nestin-cre/Cx43$^{flox/flox}$ animals cannot manufacture this ocular fluid, a progressive lenticular failure would be predicted to begin at eye opening.

Other features of the ocular phenotype are not understood. For example, it is not clear why the posterior pigment epithelium (PPE) separated from the anterior myoepithelium (AME). There have been indications in other experimental systems that interruption of gap junctional intercellular communication can result in loss of cell-cell adhesion and delamination of epithelial cells (Paul et al., 1995). Thus, alterations in cell adhesion may underlie this ocular phenotype. In the monkey, gap junctions are known to join cells within the planes of both the AME and PPE, in addition to joining the two epithelia at their apical surfaces, analogous to the ciliary epithelium (Freddo, 1984). Since we observed abundant Cx43 immunohistochemical signal in these cells (Fig. 6C,D), some of the junctions described in the literature (Freddo, 1984) certainly contain Cx43. However, a complete inventory of connexins in the iris is not yet available. Nevertheless, given that the AME and PPE of the iris share a common embryological lineage with the PE and NPE of the ciliary epithelium, it is tempting to speculate that the AME and PPE are also joined apex-to-apex by Cx43, and that loss of this connexin is mechanistically involved with the iridal splitting.

Permeability of HRP in the iris has been studied in the rhesus monkey, and tight junctions between the posterior pigmented epithelial cells block the diffusion of HRP migrating into the iridal stroma from the posterior chamber (Freddo, 1984). As the blood vessels in the iris do not leak plasma proteins (Freddo and Raviola, 1982), tight junctions between the PPE cells may also function to block leakage of aqueous humor back into the iridal stroma from the posterior chamber. The origin of the precipitate in the pathological space between the AME and PPE is not understood. As there are no tight junctions between the AME cells, the stroma of the ciliary body might be a source. However, since a protein precipitate is seen on both the basal (posterior chamber side) and apical (newly formed pathological space) sides of the PPE, it is not possible to assess the barrier function of the tight junctions in this epithelium.

Contraction of the iridal sphincter with meiosis may have been due to the unopposed action of the sphincter following loss of Cx43 from the anterior myoepithelium (the dilator of

the iris). We observed a complete loss of Cx43 from the iridal epithelia, and this may have interfered with the coordinated function of the myoepithelial cells. As the arterioles in the nestin-*cre*/Cx43$^{flox/flox}$ iris did not appear dilated relative to controls, we provisionally conclude that sympathetic innervation to the region was not compromised, which would also have resulted in relaxation of the dilator. These issues will need more detailed study before more definitive conclusions can be drawn.

Materials and Methods

Mice

The generation of the Cx43$^{flox/flox}$ mice has been described previously (Liao et al., 2001). The nestin-*cre* transgenic line was obtained from The Jackson Laboratory (Bar Harbor, ME). The ROSA26 reporter mouse was obtained from Dr Susan Dymecki (Department of Genetics, Harvard Medical School). Littermate Cre-positive, Cx43$^{flox/+}$ heterozygotes were used as controls in all experiments unless otherwise indicated. Mice were housed and cared according to institutional guidelines.

PCR analysis

Mice were genotyped by PCR (Irwin et al., 1996). Primer sequences were as follows: Cre: 5′-atttgcctgcattaccggtc-3′ and 5′-atcaacgttttcttttcgga-3′; ROSA26-lacZ reporter: 5′-ccgacggcacgctgattgaag-3′ and 5′-atgcggtcgcgttcggttgc-3′; Cx43 wild type and floxed (PCR products of 490 and 580 bp, respectively): 5′-ctttgactctgattacagagcttaa-3′ and 5′-gtctcactgttacttaacagcttga-3′.

β-Galactosidase histochemistry

To determine the expression pattern of nestin-*cre* in the mouse eye, nestin-*cre*/ROSA26 or ROSA26 control littermate mice were anesthetized with 5-10 μl of 100 mg ml^{-1} ketamine and perfused intracardially first with Ame's medium (pH 7.4; Sigma, MO) containing 10 units ml^{-1} heparin, and subsequently with 4% paraformaldehyde in Sorenson's buffer (pH 7.4). Eyes were removed, post-fixed for 4 hours in 1% glutaraldehyde, washed 3× for 10 minutes with PBS and incubated overnight at 4°C in 20% sucrose in PBS, then frozen in OCT by immersion in liquefied propane/N_2. For histochemical detection of β-galactosidase activity, 14 μm frozen sections were prepared. Sections were incubated at 37°C with 1 mg ml^{-1} X-gal, 2 mM $MgCl_2$, 0.1% sodium deoxycholate, 0.02% NP-40, 5 mM potassium ferrocyanide, and 5 mM potassium ferricyanide in phosphate buffer pH 7.3 (Schilling et al., 1991). Light micrographs were captured using a Spot RT camera mounted on a Nikon E800 photomicroscope.

Immunofluorescence

Mice were euthanized by CO_2 inhalation followed by decapitation. Eyes were fixed by immersion in 4% paraformaldehyde in PBS (pH 7.4) overnight at 4°C then rinsed in PBS, dehydrated, embedded in paraffin, sectioned (5 μm) and mounted. Some slides were stained with Hematoxylin and Eosin (H and E). For immunostaining, slides were deparaffinized, treated with proteinase K for 5 minutes at 37°C and then blocked in 5% serum, 1% bovine serum albumin, 0.1% Tween-20 in PBS (pH 7.4) for 1 hour. Sections were incubated with rabbit anti-Cx43 antibody (1:1000; Sigma, raised against residues 363-382) overnight at 4°C, and stained with Cy3 goat anti-rabbit (1:400; Chemicon, Temecula, CA) for 1 hour at room temperature. As the Sigma antibody gave an unexpected Cx43 signal in lens fibers, we tested the specificity of this antibody on eyes collected from E15, Cx43 KO embryos originating from mating heterozygous Cx43$^{+/-}$ mice. Tail biopsy specimens from individual embryos were collected and genotyped by PCR as described previously (White et al., 2001).

Lens capsules were harvested, fixed as indicated above and immunostained with anti-Cx43 antibodies from Chemicon (1:500; Temecula, CA) and Invitrogen/Zymed (1:300; San Francisco, CA). In additional control studies, eyes were collected and fixed as above, but were frozen in OCT by immersion in liquefied propane/N_2. Frozen sections of WT and *cre* expressing specimens obtained with a Microm HM 500 OM cryostat were then blocked as above and stained with anti-Cx43 obtained from Chemicon (Temecula, CA; raised against residues 252-270) and Invitrogen/Zymed (San Francisco, CA; raised against the third cytoplasmic domain). For studies of Cx40 distribution, specimens were fixed and frozen sectioned as above and stained with anti-Cx40 reagents (Simon et al., 1998) and the Cx40-A antibody from Alpha Diagnostic International (San Antonio, TX).

Images were collected with a Nikon E800 photomicroscope equipped with a SPOT-2 digital camera. 5 Mb TIFF images were collected and contrast optimized in Photoshop. Image collages were assembled and labeled in CorelDraw, then exported as final JPEG files.

Horseradish peroxidase (HRP) and electron microscopy (EM)

Mice were anesthetized with 5-10 μl of 100 mg ml^{-1} ketamine, the abdominal cavity opened and the inferior vena cava injected with 0.1 ml of a 20 mg ml^{-1} solution of HRP (Type II, Sigma) in PBS warmed to 37°C over 1 minute. After 5 minutes, animals were sacrificed and the eyes enucleated. The posterior half of the globe was cut away with scissors in fixative (4% formaldehyde, 2.5% glutaraldehyde, 2% $CaCl_2$, 0.1 M cacodylate buffer, pH 7.4). The lens was removed by cutting the zonular fibers. The peroxidase reaction was carried out as described by Raviola (Raviola, 1974). Specimens were embedded in Epoxy resins and 0.5 μm and 70 nm sections were cut for light and electron microscopy. Light microscope sections were counterstained with 0.1% toluidine blue; electron microscope sections were studied either unstained or following routine lead citrate. All electron micrographs were collected using a JEOL 1200EX at 80 KV using both conventional and digital plates.

Analysis of aqueous humor

Three-week-old mice were euthanized by CO_2 inhalation followed by decapitation. Using a micromanipulator, a glass pipette with a tip broken to 2 μm diameter was introduced into the anterior chamber through the cornea of the eye in situ. The pipette was attached to a vacuum pump valved with a Picospritzer (General Valve Corp., Fairfield, NJ) permitting 5 millisecond pulses of suction to the back of the pipette. Aqueous humor was withdrawn until the cornea was observed to buckle using a dissecting microscope. In general, 5 μl of clear aqueous could be retrieved from each eye. Equal volumes of aqueous from *cre*$^{+}$/Cx43$^{+/flox}$ and Cx43$^{flox/flox}$ eyes were diluted with 2× SDS sample buffer and SDS-PAGE was performed as described previously (White et al., 1998). Prominent bands were excised from the gels following visualization by silver staining (Bio-Rad; Hercules, CA) and analyzed by Mass Spectroscopy at the Department of Cell Biology Taplin Biological Mass Spectrometry Facility using a LCQ DECA ion-trap mass spectrometer (ThermoFinnigan).

The authors have no conflict of interest with any of the data presented in this paper. We are grateful to Alex Simon for providing the Cx40$^{-/-}$ eyes. Helpful discussions with Elio Raviola are highly appreciated. This work is supported by grants EY02430 (D.A.G.), GM37751 and EY14127 (D.L.P.) and HL12792 and HL23531 (B.R.D.) from the NIH.

References

Avila, M. Y., Stone, R. A. and Civan, M. M. (2002). Knockout of A3 adenosine receptors reduces mouse intraocular pressure. *Invest. Ophthalmol. Vis. Sci.* **43**, 3021-3026.

Civan, M. M. and Macknight, A. D. (2004). The ins and outs of aqueous humour secretion. *Exp. Eye Res.* **78**, 625-631.

Coffey, K. L., Krushinsky, A., Green, C. R. and Donaldson, P. J. (2002). Molecular profiling and cellular localization of connexin isoforms in the rat ciliary epithelium. *Exp. Eye Res.* **75**, 9-21.

Debeer, P., Van Esch, H., Huysmans, C., Pijkels, E., De Smet, L., Van de Ven, W., Devriendt, K. and Fryns, J. P. (2005). Novel *GJA1* mutations in patients with oculo-dento-digital dysplasia (ODDD). *Eur. J. Med. Genet.* **48**, 377-387.

Do, C. W. and To, C. H. (2000). Chloride secretion by bovine ciliary epithelium: a model of aqueous humor formation. *Invest. Ophthalmol. Vis. Sci.* **41**, 1853-1860.

Do, C. W. and Civan, M. M. (2004). Basis of chloride transport in ciliary epithelium. *J. Membr. Biol.* **200**, 1-13.

Flenniken, A. M., Osborne, L. R., Anderson, N., Ciliberti, N., Fleming, C., Gittens, J. E., Gong, X. Q., Kelsey, L. B., Lounsbury, C., Moreno, L. et al. (2005). A *Gja1* missense mutation in a mouse model of Oculodentodigital Dysplasia (ODDD). *Development* **132**, 4375-4386.

Freddo, T. F. (1984). Intercellular junctions of the iris epithelia in *Macaca mulatta*. *Invest. Ophthalmol. Vis. Sci.* **25**, 1094-1104.

Freddo, T. F. and Raviola, G. (1982). Freeze-fracture analysis of the interendothelial junctions in the blood vessels of the iris in Macaca mulatta. *Invest. Ophthalmol. Vis. Sci.* **23**, 154-167.

Irwin, M. H., Moffatt, R. J. and Pinkert, C. A. (1996). Identification of transgenic mice by PCR analysis of saliva. *Nat. Biotechnol.* **14**, 1146-1148.

Ito, M. and Yoshioka, M. (1999). Regression of the hyaloid vessels and pupillary membrane of the mouse. *Anat. Embryol. Berl.* **200**, 403-411.

Karnovsky, M. J. (1967). The ultrastructural basis of capillary permeability studied with peroxidase as a tracer. *J. Cell Biol.* **35**, 213-236.

Liao, Y., Day, K. H., Damon, D. N. and Duling, B. R. (2001). Endothelial cell-specific knockout of connexin 43 causes hypotension and bradycardia in mice. *Proc. Natl. Acad. Sci. USA* **98**, 9989-9994.

Loddenkemper, T., Grote, K., Evers, S., Oelerich, M. and Stogbauer, F. (2002). Neurological manifestations of the oculodentodigital dysplasia syndrome. *J. Neurol.* **249**, 584-595.

Mayer, E. J., Hughes, E. H., Carter, D. A. and Dick, A. D. (2003). Nestin positive cells in adult human retina and in epiretinal membranes. *Br. J. Ophthalmol.* **87**, 1154-1158.

McLaughlin, C. W., Peart, D., Purves, R. D., Carre, D. A., Macknight, A. D. and Civan, M. M. (1998). Effects of HCO_3^- on cell composition of rabbit ciliary epithelium: a new model for aqueous humor secretion. *Invest. Ophthalmol. Vis. Sci.* **39**, 1631-1641.

Mitchell, C. A., Risau, W. and Drexler, H. C. (1998). Regression of vessels in the tunica

vasculosa lentis is initiated by coordinated endothelial apoptosis: a role for vascular endothelial growth factor as a survival factor for endothelium. *Dev. Dyn.* **213**, 322-333.
Oh, J., Krupin, T., Tang, L. Q., Sveen, J. and Lahlum, R. A. (1994). Dye coupling of rabbit ciliary epithelial cells in vitro. *Invest. Ophthalmol. Vis. Sci.* **35**, 2509-2514.
Paul, D. L., Yu, K., Bruzzone, R., Gimlich, R. L. and Goodenough, D. A. (1995). Expression of a dominant negative inhibitor of intercellular communication in the early *Xenopus* embryo causes delamination and extrusion of cells. *Development* **121**, 371-381.
Paznekas, W. A., Boyadjiev, S. A., Shapiro, R. E., Daniels, O., Wollnik, B., Keegan, C. E., Innis, J. W., Dinulos, M. B., Christian, C., Hannibal, M. C. et al. (2003). Connexin 43 (*GJA1*) mutations cause the pleiotropic phenotype of oculodentodigital dysplasia. *Am. J. Hum. Genet.* **72**, 408-418.
Pearson, R. A., Dale, N., Llaudet, E. and Mobbs, P. (2005). ATP released via gap junction hemichannels from the pigment epithelium regulates neural retinal progenitor proliferation. *Neuron* **46**, 731-744.
Raviola, E., Goodenough, D. A. and Raviola, G. (1980). Structure of rapidly frozen gap junctions. *J. Cell Biol.* **87**, 273-279.
Raviola, G. (1974). Effects of paracentesis on the blood-aqueous barrier: an electron microscope study on Macaca mulatta using horseradish peroxidase as a tracer. *Invest. Ophthalmol. Vis. Sci.* **13**, 828-858.
Raviola, G. (1976). Blood-aqueous barrier can be circumvented by lowering intraocular pressure. *Proc. Natl. Acad. Sci. USA* **73**, 638-642.
Raviola, G. and Raviola, E. (1978). Intercellular junctions in the ciliary epithelium. *Invest. Ophthalmol. Vis. Sci.* **17**, 958-981.
Reaume, A. G., De Sousa, P. A., Kulkarni, S., Langille, B. L., Zhu, D., Davies, T. C., Juneja, S. C., Kidder, G. M. and Rossant, J. (1995). Cardiac malformation in neonatal mice lacking connexin43. *Science* **267**, 1831-1834.
Rohde, E., Tomlinson, A. J., Johnson, D. H. and Naylor, S. (1998). Comparison of protein mixtures in aqueous humor by membrane preconcentration – capillary electrophoresis – mass spectrometry. *Electrophoresis* **19**, 2361-2370.
Ruiz-Ederra, J. and Verkman, A. S. (2006). Mouse model of sustained elevation in intraocular pressure produced by episcleral vein occlusion. *Exp. Eye Res.* **82**, 879-884.
Schilling, K., Dickinson, M. H., Connor, J. A. and Morgan, J. I. (1991). Electrical activity in cerebellar cultures determines Purkinje cell dendritic growth patterns. *Neuron* **7**, 891-902.
Simon, A. M., Goodenough, D. A. and Paul, D. L. (1998). Mice lacking connexin40 have cardiac conduction abnormalities characteristic of atrioventricular block and bundle branch block. *Curr. Biol*. **8**, 295-298.
Soriano, P. (1999). Generalized lacZ expression with the ROSA26 Cre reporter strain. *Nat. Genet.* **21**, 70-71.
Stelling, J. W. and Jacob, T. J. (1997). Functional coupling in bovine ciliary epithelial cells is modulated by carbachol. *Am. J. Physiol*. **273**, C1876-C1881.
Thuret, S., Alavian, K. N., Gassmann, M., Lloyd, C. K., Smits, S. M., Smidt, M. P., Klein, R., Dyck, R. H. and Simon, H. H. (2004). The neuregulin receptor, ErbB4, is not required for normal development and adult maintenance of the substantia nigra pars compacta. *J. Neurochem.* **91**, 1302-1311.
Vasconcellos, J. P., Melo, M. B., Schimiti, R. B., Bressanim, N. C., Costa, F. F. and Costa, V. P. (2005). A novel mutation in the *GJA1* gene in a family with oculodentodigital dysplasia. *Arch. Ophthalmol*. **123**, 1422-1426.
Walker, V. E., Stelling, J. W., Miley, H. E. and Jacob, T. J. (1999). Effect of coupling on volume-regulatory response of ciliary epithelial cells suggests mechanism for secretion. *Am. J. Physiol*. **276**, C1432-C1438.
White, T. W., Goodenough, D. A. and Paul, D. L. (1998). Targeted ablation of connexin50 in mice results in microphthalmia and zonular pulverulent cataracts. *J. Cell Biol.* **143**, 815-825.
White, T. W., Sellitto, C., Paul, D. L. and Goodenough, D. A. (2001). Prenatal lens development in connexin43 and connexin50 double knockout mice. *Invest. Ophthalmol. Vis. Sci.* **42**, 2916-2923.
Wolosin, J. M., Candia, O. A., Petersonyantorno, K., Civan, M. M. and Shi, X. P. (1997). Effect of heptanol on the short circuit currents of cornea and ciliary body demonstrates rate limiting role of heterocellular gap junctions in active ciliary body transport. *Exp. Eye Res.* **64**, 945-952.
Yamaguchi, Y., Watanabe, T., Hirakata, A. and Hida, T. (2006). Localization and ontogeny of aquaporin-1 and -4 expression in iris and ciliary epithelial cells in rats. *Cell Tissue Res.* **325**, 101-109.
Yang, J., Bian, W., Gao, X., Chen, L. and Jing, N. (2000). Nestin expression during mouse eye and lens development. *Mech. Dev.* **94**, 287-291.
Yeh, H. I., Dupont, E., Coppen, S., Rothery, S. and Severs, N. J. (1997). Gap junction localization and connexin expression in cytochemically identified endothelial cells of arterial tissue. *J. Histochem. Cytochem.* **45**, 539-550.

Journal of Cell Science